Primary Cilia in Amacrine Cells in Retinal Development

Ke Ning,[1] Brent E. Sendayen,[1,2] Tia J. Kowal,[1] Biao Wang,[1] Bryan W. Jones,[3] Yang Hu,[1] and Yang Sun[1,2]

[1]Department of Ophthalmology, Stanford University School of Medicine, Palo Alto, California, United States
[2]Palo Alto Veterans Administration, Palo Alto, California, United States
[3]Moran Eye Center, University of Utah, Salt Lake City, Utah, United States

Correspondence: Yang Sun, 1651 Page Mill Rd, Rm 2220, Palo Alto, CA 94305, USA;
yangsun@stanford.edu.

Purpose. Primary cilia are conserved organelles found in polarized cells within the eye that regulate cell growth, migration, and differentiation. Although the role of cilia in photoreceptors is well-studied, the formation of cilia in other retinal cell types has received little attention. In this study, we examined the ciliary profile focused on the inner nuclear layer of retinas in mice and rhesus macaque primates.

Methods. Retinal sections or flatmounts from Arl13b-Cetn2 tg transgenic mice were immunostained for cell markers (Pax6, Sox9, Chx10, Calbindin, Calretinin, ChaT, GAD67, Prox1, TH, and vGluT3) and analyzed by confocal microscopy. Primate retinal sections were immunostained for ciliary and cell markers (Pax6 and Arl13b). Optical coherence tomography (OCT) and ERGs were used to assess visual function of Vift88 mice.

Results. During different stages of mouse postnatal eye development, we found that cilia are present in Pax6-positive amacrine cells, which were also observed in primate retinas. The cilia of subtypes of amacrine cells in mice were shown by immunostaining and electron microscopy. We also removed primary cilia from vGluT3 amacrine cells in mouse and found no significant vision defects. In addition, cilia were present in the outer limiting membrane, suggesting that a population of Müller glial cells forms cilia.

Conclusions. We report that several subpopulations of amacrine cells in inner nuclear layers of the retina form cilia during early retinal development in mice and primates.

Keywords: amacrine cell, ARL13B, eye, Müller glia, Pax6, primary ciliary retina, VGLUT3

Primary cilia are microtubule-based organelles that project from the surface in postmitotic mammalian cells.[1,2] In many cell types, primary cilia can function as a cellular antenna to sense external cues and transduce intracellular signaling involved in diverse cellular processes during development.[1,3–6] Essential to central nervous system development, primary cilia are required for tissue patterning, neuronal migration, learning, and memory formation.[7–10] Defects of cilia in humans can result in a group of conditions called ciliopathies, that present in the brain, kidneys, and eyes.[11–15] During eye development, cilia exhibit dynamic behavior during early retinal differentiation and play roles in proliferation and survival of retinal progenitors.[16,17] In humans, disruption of key ciliary genes can result in anophthalmia or microphthalmia.[18–20] It was also shown that proper ciliogenesis is critical for eye patterning and morphogenesis in mouse.[16,21]

In the eye, the connecting cilium of the photoreceptors has garnered the most attention. Outer segments of photoreceptors are highly modified primary cilia responsible for the trafficking of opsins to distal portions of rods and cones.[22,23] Defects in the structure and function of photoreceptor cilia can result in progressive retinal degeneration, leading to irreversible blindness.[24–26] Retinal ganglion cell (RGC) cilia have recently been described as required for RGC formation during development and can enhance cell survival after optic nerve crush.[17,27] In early electron microscopy reports, other retinal cells were also noted to express primary cilia in vertebrate retinas.[28–31] Bipolar cells receive synaptic input from photoreceptors and transfer visual information to amacrine and ganglion cells[32,33]; primary cilia have been described in bipolar cells in guinea pig and human retinas using electron microscopy.[28,29]

Amacrine cells were also found to express cilia in cat and rabbit retinas using the Richardson silver stain.[28,29] Amacrine cells are interneurons located in the inner nuclear layer (INL), modulating and shaping the information transmitted from bipolar to ganglion cells.[34,35] Amacrine cells play a role in encoding and integrating numerous complex features of the visual world.[36,37] Many different types of amacrine cells have been identified in the INL; the majority are inhibitory interneurons, which release inhibitory neurotransmitters, gamma-aminobutyric acid, or glycine.[38,39] vGluT3 amacrine cells release both glutamate and glycine and respond to object and image motion.[40,41]

Another class of retinal cells is the Müller cells, whose cell bodies reside in the INL. Müller cells project across the entire retina as structural, metabolic, and homeostatic support structures.[42,43] Isolated Müller cells from rats have been shown to have cilia and play a role in proliferation and dedifferentiation.[44] However, the temporal and spatial distribution of primary cilia in the INL during retinal

development in rodents is not clear, especially in the postnatal development stage.

Despite the previous detection of cilia in other nonphotoreceptor retinal cells, a thorough characterization of cilia on these cells during retinal development and in the adult stage in rodents has yet to be conducted. We investigated the localization and expression of primary cilia in neurosensory retina of mice and primates. Using immunofluorescence with ciliary markers and ultrastructural analysis of several types of mammalian retinas, we show a differential expression of cilia in mice and primates.

METHODS

Reagents

Details for antibodies and their conditions of use are as follows: anti-Arl13b mouse antibody (IF: 1:2000) was purchased from Antibodies Inc (Davis, CA; N295B/66); anti-Pax6 mouse antibody (IF: 1:500), anti-Chx10 chicken antibody (IF: 1:500), and anti-Sox9 rabbit antibody (IF: 1:500) were purchased from Abcam (kindly provided by Dr Jeffrey Goldberg, Stanford, CA); anti-Calretinin rabbit antibody (IF: 1:500) and anti–tyrosine hydroxylase (TH) rabbit antibody (IF: 1:500) were purchased from Proteintech (Chicago, IL; 12278-1-AP; 25859-1-AP); anti-choline acetyltransferase (ChAT) rabbit antibody (IF: 1:500), anti-GAD67 mouse antibody (IF: 1:500), anti-Calbindin mouse antibody (IF: 1:500) and anti-Vglut3 Guinea Pig antibody (IF: 1:500) were purchased from Millipore Sigma (Burlington, MA; AB143; MAB5406; C9848; AB5421-I); anti-Prox1 rabbit antibody (IF: 1:500) was purchased from BioLegend (Dedham, MA; 925202); The primary antibodies were detected using AlexaFluor 488, 647 and 594 IgG secondary antibodies (IF: 1:200, obtained from Life Technologies, Carlsbad, CA). ProLong Gold Antifade Mount and DAPI were purchased from Invitrogen (Waltham, MA).

Animals

Eyes from C57BL/6J and Tg (CAG-Arl13b/mCherry)1Kvand Tg (CAG-EGFP/CETN2)3-136 4Jgg/KvandJ (referred to as Arl13b-Cetn2 tg, Jackson Laboratory #027967) were used in this study. Primary cilia are labeled with fluorescent protein mCherry targeting Arl13b protein and GFP labeled Centrin2 in Arl13b-Cetn2 tg mice.[45] V*ift88* mice were generated by breeding Vglut3-Cre (Vglut3-IRES2-Cre-D mice, Jackson Laboratory #028534) and IFT88f/f (Jackson Laboratory #022409) transgenic lines to create Vglut3-expressing cells-specific IFT88 knockouts. Primers for genotyping were: VGLUT3, forward: CATCAGAAACCTGGACTCTG; reverse: AGGCTCCAGAAACAGTCTAACG; Internal Pos Ctrl CETN-GFP, forward: CTAGGCCACAGAATTGAAAGATCT, reverse: GTAGGTGGAAATTCTAGCATCATCC. Mice were maintained under a 12:12 hour light–dark cycle in the animal facility. All procedures followed the guidelines of the ARVO Statement for the Use of Animals in Ophthalmic and Vision Research, and all animal experiments were approved by the Institutional Animal Care and Use Committee (IACUC) of Stanford University School of Medicine. All protocols for the electron microscopy images of mouse retina were in accord with Institutional Animal Care and Use protocols of the University of Utah, the ARVO Statement for the Use of Animals in Ophthalmic and Visual Research, and the Policies on the Use of Animals and Humans in Neuroscience Research of the Society for Neuroscience. Mice were sacrificed at different postnatal ages by CO_2 inhalation before cervical dislocation. Eyes were enucleated and fixed in freshly made 4% (w/v) paraformaldehyde (PFA), 10 mM sodium periodate, 75 mM lysine in 0.1 M sodium phosphate buffer for 1 hour at room temperature. Macaque monkey retinas were obtained from terminally anesthetized macaque monkeys used in unrelated experiments.[46] The peripheral retina was then sectioned at 15 µm thickness using a cryostat (CM1860, Leica Biosystems, Wetzlar, Germany).

Retinal Flatmount

For mouse retina flatmount experiments, eyes were enucleated after perfusion with 4% PFA (in PBS) and immersed in 4% PFA fixation for 1 hour before removal of the anterior segment (cornea, iris and ciliary body, and lens). Four radical cuts were generated from the edge of the retinal cup to the equator. After careful removal of RPE/choroid/sclera layer, the remaining retinal cups were thoroughly washed in 1× PBS and processed for immunofluorescence staining.

Immunofluorescence Staining

Fixed retinal cups were washed in PBS three times for 10 minutes each, then incubated in 30% sucrose in PBS overnight at 4 °C on a nutator. After overnight incubation, eyecups were embedded in OCT media and sectioned into 10- to 15-µm slices for immunohistochemistry. Mounted retinal sections or retina cups were washed with PBS three times and incubated for 1 hour in blocking buffer containing 10% goat serum and 0.3% Triton X-100 at room temperature. After blocking, retinal sections or retinal cups were incubated with primary antibodies at 4°C overnight. After washes in PBS, sections or retinal cups were incubated in the blocking buffer containing secondary antibodies for 1 hour at room temperature. Nuclei were stained with DAPI stain. Slides or flatmounts were then washed three times with PBS and mounted with ProLong Gold (Life Technologies) on coverslips. Imaging was performed with a Zeiss LSM880 confocal microscope. For subtype of amacrine cells, six retinas were collected from perfused adult transgenic mice, Arl13b-mCherry::Centrin2-GFP, in which the primary cilia are fluorescently labeled. Each retina was cut into six fragments to facilitate whole mount staining and analysis.

Electron Microscopy

Retinal tissue for electron microscopy was collected from a 5-month-old female C57BL/6J mouse. The mouse was euthanized with isoflurane followed by cervical transection, and the eyes were enucleated. The eyes were injected with 2.5% glutaraldehyde, 1% PFA, then immersion fixed overnight in the same fixative. Tissues were dehydrated in graded methanols and osmicated. Retinal tissue was subsequently serial sectioned at 70- to 90-nm onto a polyvinyl formal resin–coated gold slot grids. Each section was imaged by automated transmission electron microscopy at 2.18 nm resolution with more than 1000 image tiles per section stored in 16- and 8-bit versions, creating image pyramids for web visualization of a 0.25-mm diameter volume of the mouse retina, viewed and annotated with the Viking viewer.[47,48]

Pattern ERG (PERG)

Mice were anesthetized by mixed xylazine (0.01 mg/g) and ketamine (0.08 mg/g) as described elsewhere.[49] PERG was measured by Miami PERG system (Intelligent Hearing Systems, Miami, FL) according to published procedures.[49,50] Briefly, rodent pupils were dilated with 1% tropicamide sterile ophthalmic solution (Akorn, Somerset, NJ), followed by application of a lubricant eye drop (Systane Ultra Lubricant Eye Drops, Alcon Laboratories, Ft. Worth, TX). The reference electrode, ground electrode, and active steel needle electrode were placed as previously described.[49] The stimulus was generated by black and white moving contrast-reversing bars that were aligned with the projection of the pupil. The amplitude was measured between P1 to N2. Three mice per group and 800 reads per eye were recorded. The mean of the amplitude in the Vift88 mice was compared with that in the age-compared control mice to calculate the amplitude change.

SD-OCT Imaging

SD-OCT imaging (Heidelberg Spectralis SLO/OCT system; Heidelberg Engineering, Heidelberg, Germany) was used to visualize the retinal structure. The system has been introduced in detail in previous publications.[49] Briefly, pupils were dilated and covered with a customized +10-D contact lens (3.0 mm diameter, 1.6 mm BC, PMMA clear, Advanced Vision Technologies, Hod Hasharon, Israel). OCT scans were performed to obtain high-resolution images. The average thickness of INL and RGC was measured separately and manually with the assistance of the Heidelberg software.

Statistical Analysis

All statistical analysis was performed using Graphpad8 (Prism) software. Results are displayed as mean values ± SEM. Paired *t* tests were used for statistical analyses in comparisons of various treatments as indicated. A *P* value of less than 0.05 was considered statistically significant. The INL was viewed by confocal microscopy and three images (500 µm from the edges) per retinal segment were captured using a 63× objective. Fifty marker-positive cells were examined. Arl13b-mCherry signal was counted as a cilium if one end of the signal was directly adjacent to the Centrin2-GFP signal. All research was conducted in compliance with the ARVO Statement for the Use of Animals in Ophthalmic and Vision Research.

RESULTS

Primary Cilia Are Expressed in the INLs of the Mouse Retina

To determine the spatial and temporal patterns of primary cilia expression in retinal cells, we analyzed the ARL13B expression levels and distribution from P0 to P21 retinas in ARL13B-mcherry Centrin2-GFP double transgenic mice (Fig. 1). We traced ciliated cells on retina sections by confocal z-stack. Cilia appeared as elongated ARL13B-mcherry staining adjacent to Centrin2-GFP centrioles. A clear layer of
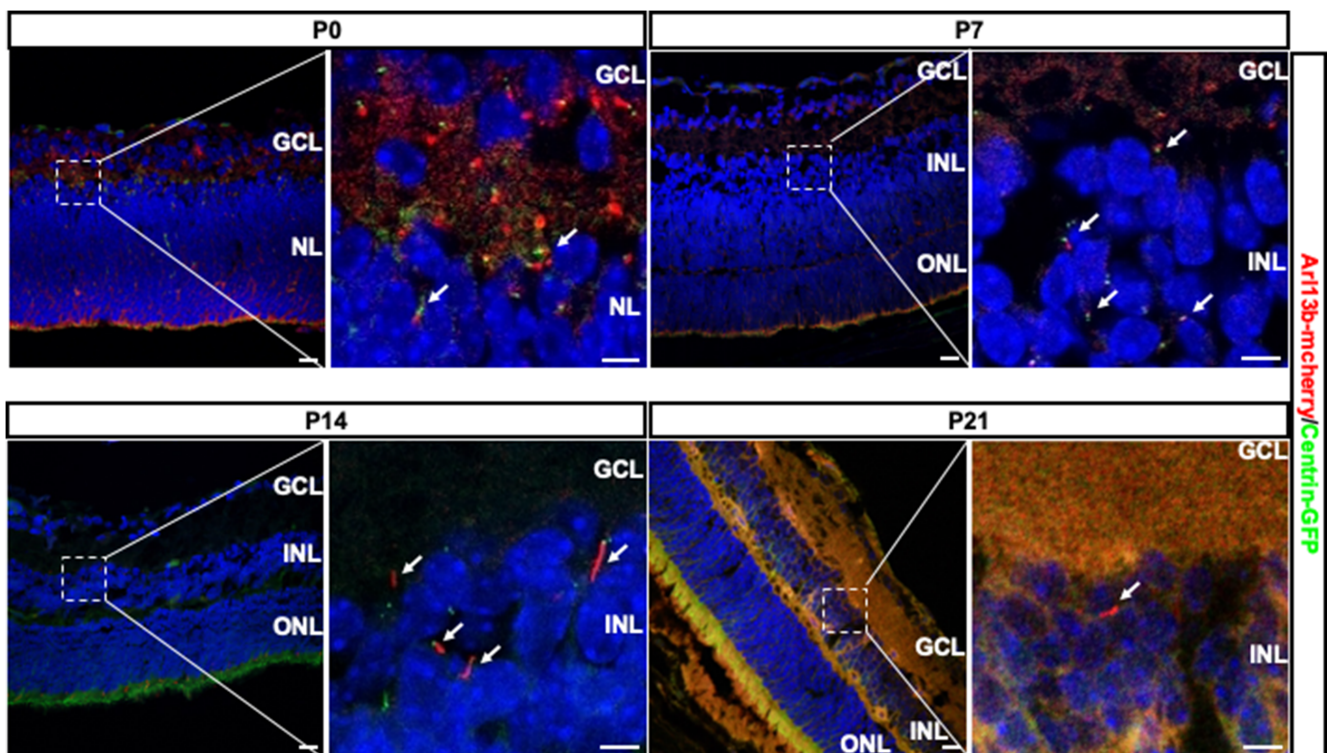

FIGURE 1. Primary cilia are expressed in INLs of the mouse retina. Localization by confocal microscopy of primary cilia in mouse retina during development. Frozen sections of retinas (10 µm) from ARL13B-mcherry Centrin2-GFP double transgenic mice at the indicated developmental stages. Nuclei are visualized with DAPI. Primary cilia are visualized by Arl13b (in *red*) and Centrin2 (in *green*). Magnified images are focused on INL of retinas. GCL, RGC layer; ONL, outer nuclear layer; RP, retinal progenitor cell. Scale bars: small 20 µm; magnified images, 100 µm. (*Arrow* marks the primary cilia).

GFP-positive centrioles was connected to cilia and mcherry positive outer segments on photoreceptors during development. At P0, most primary cilia were detected in the ganglion cell layer and the inner part of the neuroblastic layer (NL). Few primary cilia were detected in the central NL (<10%; data not shown). At P7, a distinct outer plexiform layer separated the thick NL into the photoreceptor and INL. As at P0, most of the primary cilia appeared in the inner part of the INL. Cilia were also scattered in a nonspecific pattern in the middle portion of the outer nuclear layer, and a few cilia were present in the outer INL, close to the outer plexiform layer (Fig. 1, *arrow*). By P21, the majority of primary cilia were localized in the inner part of the INL. Taken together, the expression profile of primary cilia in the inner part of the INL and ganglion cell layer of mouse retina did not change over the developmental stages that we analyzed.

Pax6-Positive Cells Contain Primary Cilia at Different Developmental Stages

Pax6 is a member of the Pax family of transcription factors that is thought to play a crucial role in the development of the eye, brain, and olfactory system.[51,52] Previous studies indicated that Pax6 may regulate progenitor cell proliferation, the timing of differentiation, and the determination of neural retina cell fate.[53] Based on these earlier reports, we hypothesized that the expression pattern of ARL13B would be consistent with that of Pax6. To examine the primary cilia distribution during retinal development, we immunostained sections with Pax6 antibody at multiple time points (Fig. 2). We observed that Pax6-positive cells consistently formed primary cilia at P0 and P7. Conversely, not all ciliated cells in the retina expressed Pax6. Interestingly, we observed that scattered primary cilia in the central NL were also Pax6 positive. We found no further changes in Pax6-positive cells containing primary cilia at P14 or P21. Together, these results suggested that primary cilia form in the INL in retinal Pax6-positive cells and are retained at later stages.

Identification of a Population of Ciliated Retinal Cells in the Outer Limiting Membrane

Müller glia are retinal supporting cells that span the entire retina from the inner limiting to the outer limiting membrane.[43] In mice, Müller glia possess the capacity for regeneration and act as retinal stem cells.[42] In the present study, we observed that the retina of ARL13B-mcherry Centrin2-GFP double transgenic mice contained a group of primary cilia located close to the outer limiting membrane. Importantly, previous studies hypothesized that this group of primary cilia belongs to Müller glia.[22,54] To test this hypothesis, we used a glial cell marker, sox9, to show Müller glia distribution in P21 retinas.[55–58] We observed that the number of primary cilia was less than the number of respective Müller glial cells, indicating that not all Müller glia form cilia. Because it was difficult to distinguish primary cilia in the outer limiting membrane at P0, we determined ciliary length at later stages (P7, P14, and P21) of retinal development (Fig. 3A). Interestingly, ciliary length was significantly greater at P14 than at P7 and P21 (Fig. 3B). To consolidate these data, we next analyzed the ciliation profile of retinas derived from adult rhesus macaques. We identified primary cilia in proximity to the outer limiting membrane (Fig. 3C), but Müller glia markers confirmed that not all Müller glia possess cilia. The average length of cilia in primate retinas was 1.2 µm (Fig. 4C). Taken together, these results suggest that a group of primary cilia close to the outer limiting membrane is likely to be associated with Müller glia and that the length of these cilia varies during retinal development.

Mouse Amacrine Cells That Form Cilia Are PAX6 Positive

The INL houses the cell bodies of horizontal cells, bipolar cells, amacrine cells, and Müller glial cells. We next wanted to investigate whether specific retinal cell types form primary cilia in the INL after retinal maturation. Because the distribution of horizontal cells is in the outer portions of the INL, we hypothesized that the ciliated cells are either bipolar or amacrine cells. All amacrine cells are thought to express Pax6[59]; therefore, we used an anti-Pax6 antibody to assess whether ciliated cells are amacrine cells (Fig. 4A). We observed primary cilia in cells that were positive for Pax6, suggesting that amacrine cells form primary cilia. In addition, the staining of rhesus macaque retina for Pax6 and ciliary markers revealed the presence of primary cilia in amacrine cells of adult primates (Fig. 4B). The average length of amacrine cilia was 1.6 µm (Fig. 4C). Electron microscopy also demonstrated the presence of primary cilia in amacrine cells of adult mouse retinas (Fig. 4D). Interestingly, bipolar cells, which are placed on the outer side of the INL and characterized by Chx10 immunoactivity, were labeled with anti-Chx10 antibody.[60] The immunostaining analysis showed that bipolar cells did not form primary cilia. In conclusion, we identified amacrine cells containing primary cilia after retinal maturation.

Identification of Primary Cilia in Subtypes of Amacrine Cells in Mouse

Amacrine cells are classified into more than 30 morphologic subpopulations in the mammalian retina.[35] Our data indicated that amacrine cells form cilia in mouse and primate retinas. Next, we decided to investigate the cilia profile in subtypes of amacrine cells in mouse retinas at P33 when all the retinal cell types have completed differentiation. Retina flatmounts were stained using glutamic acid decarboxylase 67 (GAD67), calbindin, calretinin, ChaT, TH, and Prox1 antibodies to determine the fraction of ciliated cells that express various markers (Fig. 5A). The TH-positive subtype was the most common ciliated subtype in adult mouse retina (54.2 ± 31.5%), followed by the calbindin-positive subtype (57.5 ± 3.4%). Less than one-half of the GAD67-positive subtype amacrine cells (43.8 ± 6.6%), calretinin-positive subtype amacrine cells (34.6 ± 13.1%), and ChaT-positive subtype amacrine cells (35.7 ± 2.0%) expressed primary cilia. For Prox1-positive amacrine cells, only 3.3 ± 4.7% were ciliated. We further examined the ciliation in developmental stage in different subtypes of mouse amacrine cells. We observed significantly more ciliated TH-positive amacrine cells and Prox1-positive amacrine cells at P14. Interestingly, we observed significantly less ciliated Calbindin-positive amacrine cells at P14. There are no significant differences in ciliation of GAD67-positive, ChaT-positive, or Calretinin-positive amacrine cells between P14 and adult stages, although all of them have a trend of decreasing ciliation during development (Fig. 5B). In summary, we described the ciliary profile in different subtypes of amacrine cells both in developmental and adult stages in mice. These findings
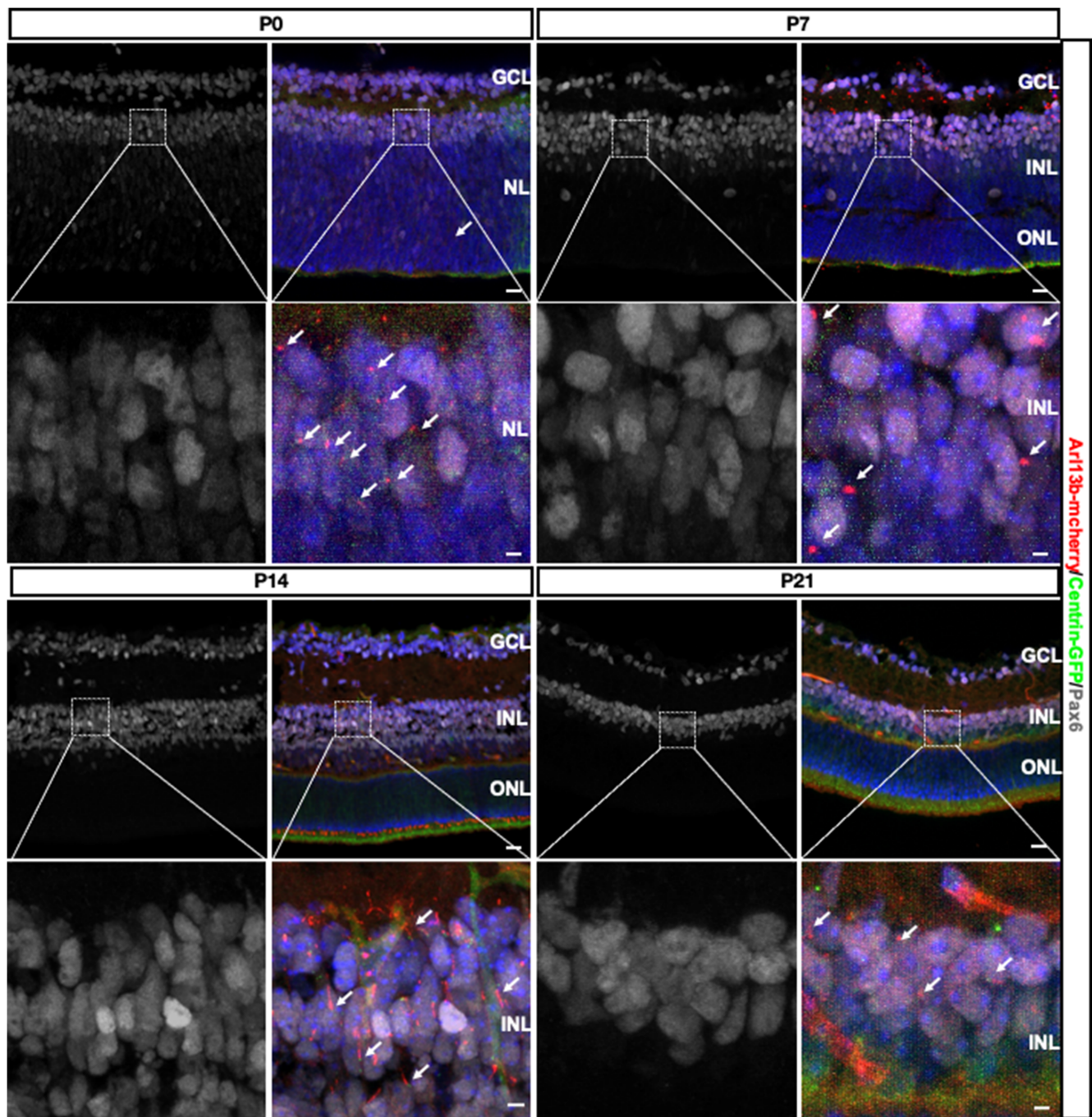
FIGURE 2. Pax6-positive cells contain primary cilia at different developmental stages. Representative images of ARL13B-mcherry Centrin2-GFP retina sections costained with Pax6 antibody (in *gray*) at different postnatal developmental stages. Frozen retinal sections were prepared (10 µm) at different stages during mouse retinal development (P0–P21). Pax6 (*gray*) immunohistochemical labeling of developmental retinas reveals its expression pattern to be localized to inner side of INL. Primary cilia labeled by Arl13b (in *red*) and Centrin2 (in *green*) show the expression pattern during retinal development with a focus on INL. Nuclei are visualized with DAPI. GCL, RGC layer; ONL, outer nuclear layer. Scale bars: P0, P7 and P21, 10 µm; P14, 20 µm. (*Arrow* marks the primary cilia).

indicate possible roles that cilia could play in retinal development, homeostasis, and diseases.

Removal of Primary Cilia in vGluT3-Expressing Amacrine Cells Did Not Affect Retinal Function

Previous reports have shown that vGluT3 amacrine cells released both glutamate and glycine and responded to object

and image motion.[40,41] To understand whether vGluT3 amacrine cells harbor cilia in mice and how cilia affect mouse vision, we first performed immunostaining with an anti-vGluT3 antibody on the cilia-GFP mouse retina at P33. We detected vGluT3-positive cells in the INL and some of the vGluT3 positive cells were also Arl13b positive, indicating that vGluT3 amacrine cells possess cilia in adult mice (Figs. 6A–C). To reveal possible retinal phenotypes arising
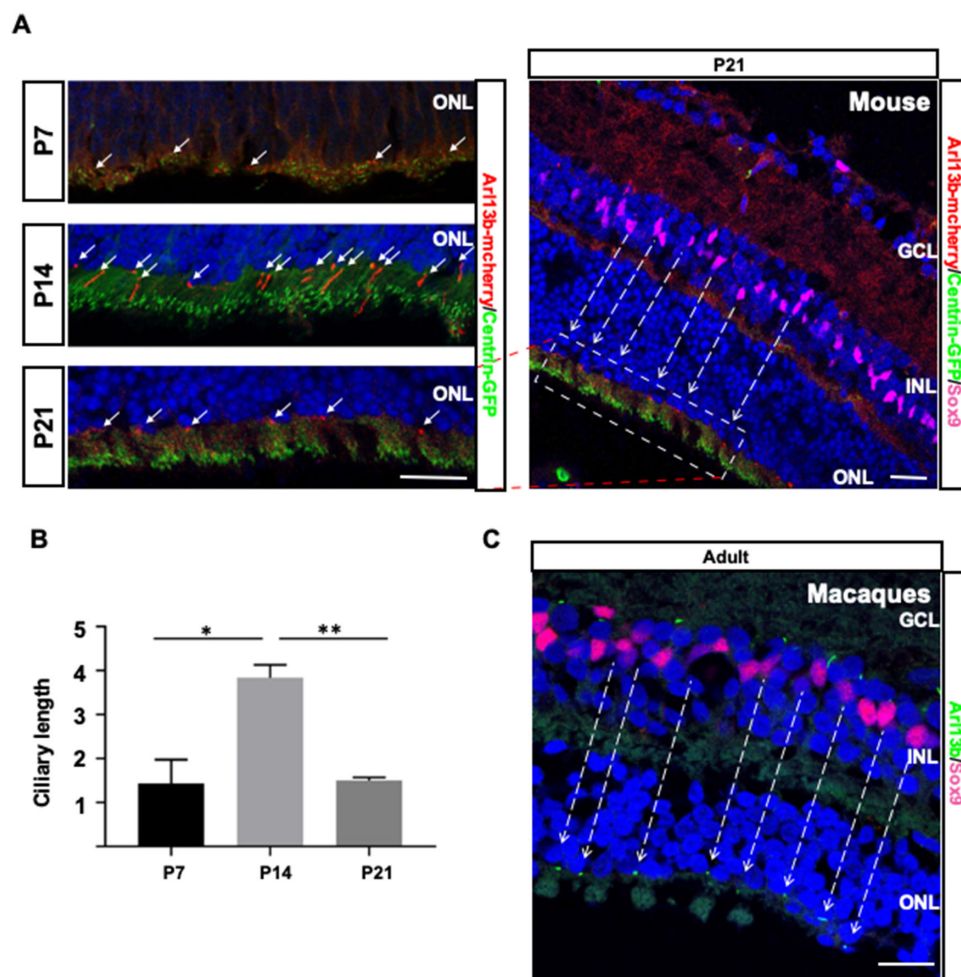
FIGURE 3. Identification of a population of ciliated retinal cells in outer limiting membrane. Detection of primary cilia on the outer limiting membrane. (**A**) High magnification images of developmental mouse retina sections (10 μm) from ARL13B-mcherry Centrin2-GFP mice show a diverse ciliary pattern in outer limiting membrane. Primary cilia are confirmed in *red* by Arl13b and in *green* by Centrin2. (**B**) Representative confocal micrographs of sections from ARL13B-mcherry Centrin2-GFP mouse retina sections at P21 costained with antibodies for Sox9 (Müller glial cell marker). Nuclei are visualized with staining by DAPI. The *white dotted line with arrowhead* indicates the possible affiliation between Müller glia and primary cilia. (**C**) Quantification of ciliary length in mouse Müller glial cells during development. Scale bar: 20 μm. (**D**) Confocal image of retina section from adult primate costained with Sox9 (*purple*), Arl13b (*red*), and Centrin2 (*green*). GCL, RGC layer; ONL, outer nuclear layer. Statistical analyses were performed using the Student *t* test; a *P* value of less than 0.05 was considered statistically significant. (*Arrow* marks the primary cilia).

in the Vift88 mice, we measured the thickness of the RGC and INL layers by OCT (Figs. 6D–F). Analysis confirmed no detectable significant changes between Vift88 mice and age-matched control mice. We also tested visual function by performing PERG in living animals (Figs. 6E–F). The result showed no significant difference in the P1 to N2 amplitude of the two groups of mice, suggesting that no deficit in vision occurred. In summary, we concluded that the absence of primary cilia in vGluT3-expressing amacrine cells did not affect retinal structures or function in adult mice.

DISCUSSION

In this study, we report the distribution of primary cilia in mouse and macaque neuroretinas. We observed the presence of numerous primary cilia in the inner side of the INL during postnatal mouse retinal development. Surprisingly, the distribution pattern of cilia is consistent with that of Pax6. These ciliated cells in adults have been identified

as amacrine cells by immunofluorescence staining and EM. We also described different cilia profiles in six subtypes of amacrine cells. Collectively, this study suggests the potentially crucial role of primary cilia in amacrine cells during development and adult homeostasis.

Primary cilia are critical for the development of vertebrate nervous systems by regulating early patterning, neuronal cell fate, and migration.[8,9] Primary cilia dysfunction leads to ocular disorders, including retinitis pigmentosa, cone dystrophies, and retinal degenerations associated with such congenital syndromes as Usher syndrome and Senior–Loken syndrome.[11,13,23,25] Defects in photoreceptor cilia are a major cause of retinal degenerative disease.[24,26] However, other ciliated retinal cell types may participate in or contribute to the progression of retinal diseases. Studies have shown that primary cilia play a role in proper patterning and morphogenesis of the optic primordium during early eye development.[16] Although previous publications have demonstrated the presence of primary cilia in the ganglion cell layer and
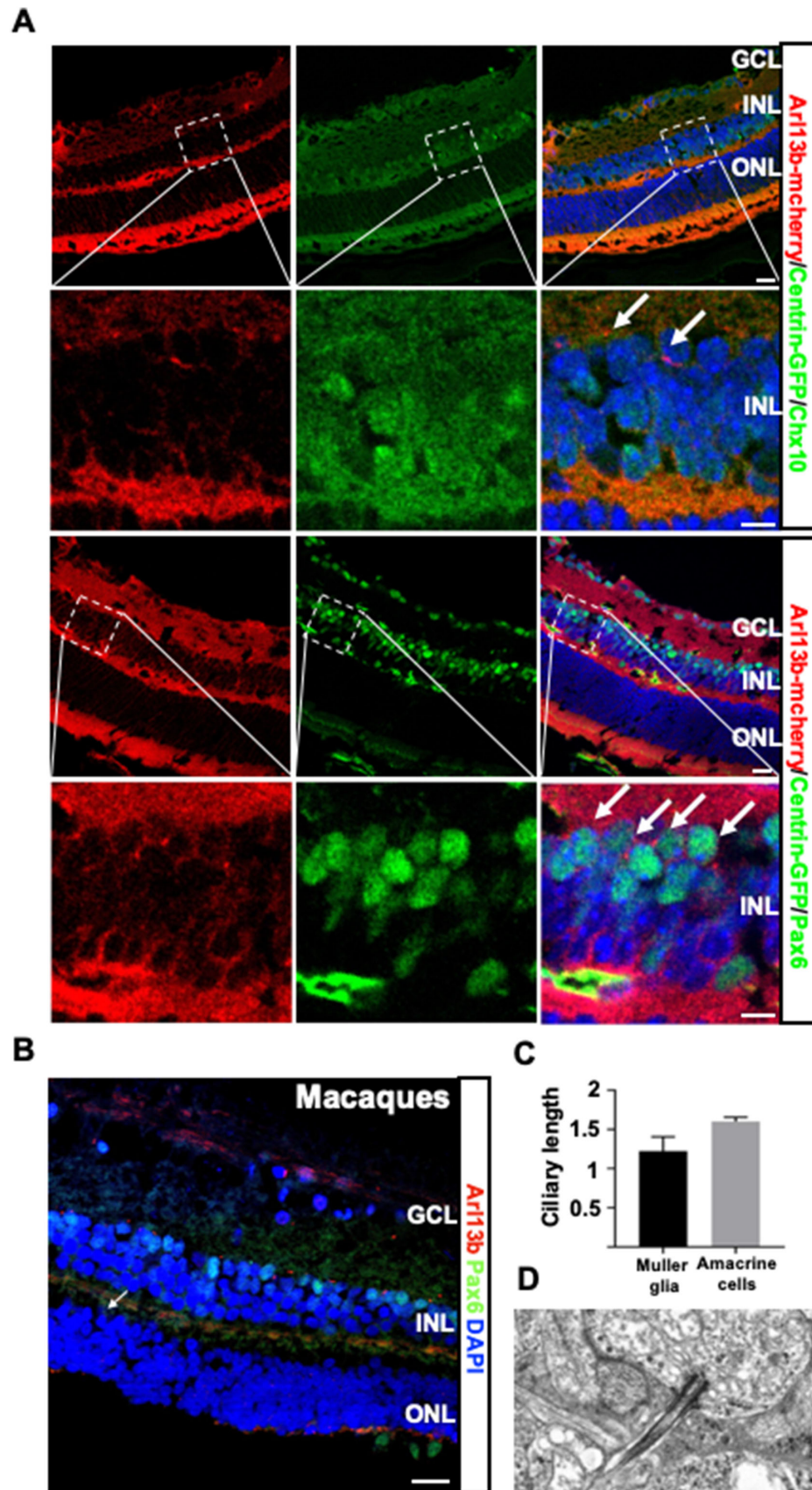
FIGURE 4. Mouse PAX6-positive amacrine cells that form cilia. Detection of primary cilia in mouse amacrine cells. (**A**) Representative confocal micrographs of retinal sections (10 μm) from ARL13B-mcherry Centrin2-GFP mice at P21 costained with antibodies targeted to cell type-specific markers. Chx10 is a well-accepted marker of bipolar cells. Pax6 is a pan-marker of all amacrine cells. Primary cilia are visualized by

Arl13b (*red*) and Centriin2 (in *green*). Nuclei are visualized with staining by DAPI. (**B**) Confocal image of retina section from adult primate (rhesus macaque) co-stained with Pax6 (*green*) and Arl13b (*red*). Colocalization of ciliary marker and Pax6-positive cells. (**C**) Quantification of ciliary length in Müller glial cells and amacrine cells in adult primate retina. (**D**) Primary cilia from a 5-month-old female C57BL/6J mouse GABAergic amacrine cell by EM (original magnification ×5000). GCL, RGC layer; ONL, outer nuclear layer. Scale bars: (**A**) small 20 µm; magnified images 100 µm; (**B**) 20 µm. (*Arrow* marks the primary cilia.) (**D**) 1 µm.
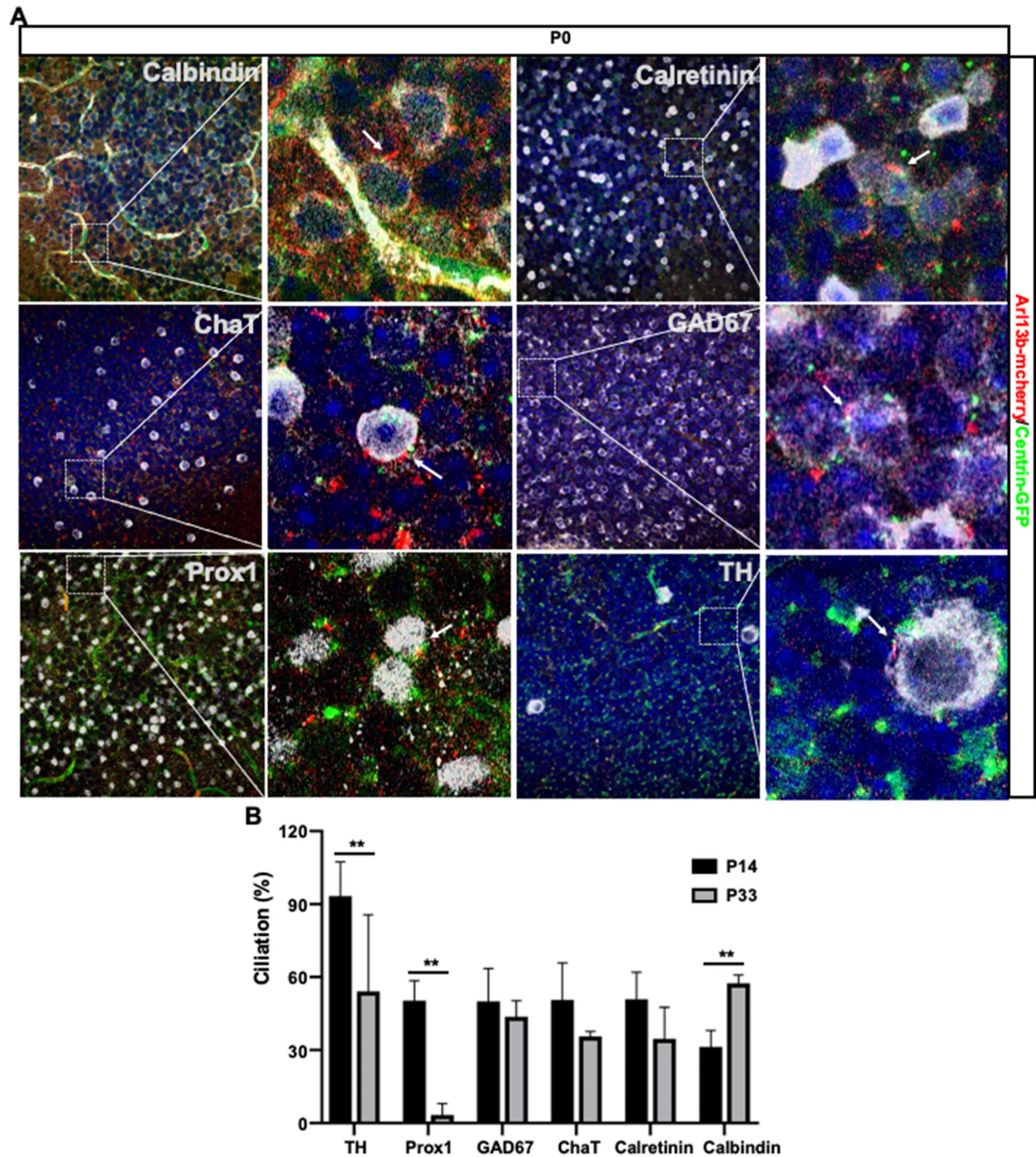

FIGURE 5. Identification of primary cilia in subtypes of amacrine cells in the mouse. Retinal flatmounts from P33 and P14 ARL13B-mcherry Centrin2-GFP mice were immunolabeled with different amacrine cells subtype-specific markers (all shown in *gray*). Confocal images were acquired by z-stacks at 0.3 µm increments and compressed into one image. (**A**) Antibodies targeted on the INL (RGC layer side) of P33 retinas and co-expressed with cilia markers (Arl13b-mCherry; Centrin2-GFP; *arrow* marks the primary cilia). Inserts show the triple-labeling at high magnification. Nuclei are visualized with DAPI. Scale bars: 20 µm. (**B**) Quantification of ciliation of six subtypes of amacrine cells both on P14 and P33 retinas ($n = 3$; $n = 6$). Statistics were analyzed using the Student t test; a P value of less than 0.05 was considered statistically significant.
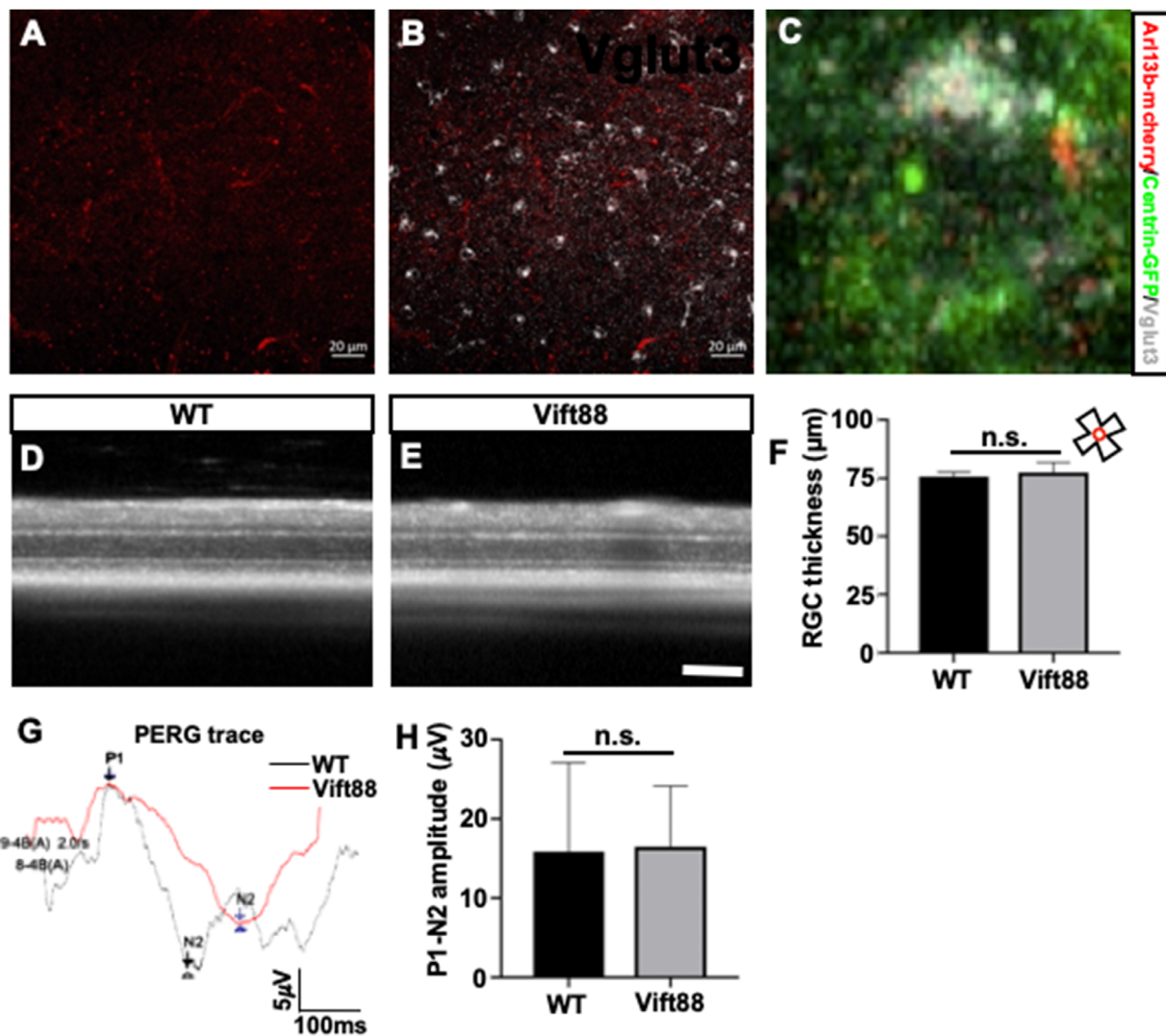
FIGURE 6. Removal of primary cilia in vGluT3-expressing amacrine cells does not affect retinal function. (**A, B**) Confocal images of retina flatmounts showing vGluT3+ amacrine cells (in *gray*) co-expressing cilia markers (Arl13b in *red* and Centrin2 in *green*) in adult ARL13B-mcherry Centrin2-GFP mice. (**C**) Inserts show the triple-labeling at high magnification. Nuclei are visualized with DAPI. (**C, D**) Representative OCT images of Vift88 retina and age-matched controls in adult mouse showing the retinal morphology. ONL; outer nuclear layer, GCL; RGC layer. (**F**) Quantification of RGC thickness ($n = 4$) in both Vift88 retina and age-matched controls. (**G**) Representative waveforms of PERG in both groups. (**H**) Quantification of P1 to N2 amplitude shows no significant difference between Vift88 and control mice ($n = 4$). Statistical analyses were performed using the Student t test; a P value of less than 0.05 was considered statistically significant. Scale bars: 20 µm.

INL in both guinea pig and human retina, the clear origin and cell types from which these cilia arise are not clear.[28] Here, we described the presence of cilia during postnatal development in the neuroretina of mice and primates.

We found that the majority of cilia are present in a group of Pax6-positive cells found in the inner part of the NL or INL during retinal development, and in amacrine cells in adulthood. Pax6 is a pleiotropic transcription factor and has been reported to be a key regulator of eye development. Dissecting the relationship between Pax6 and cilia in retina development will be an important future study. Because Pax6 is thought to be expressed in all amacrine cells as a pan-marker,[59] we then investigated whether ciliated cells are restricted to certain types of retinal cells. Our analysis of diverse types of retinal cells revealed, for the first time, that amacrine cells are distinct in expressing cilia in both mouse and macaque tissues, which is in accordance with findings

in other species.[28–30] In mouse retinas, both immunostaining and EM data have shown numerous ciliated amacrine cells. In addition, our EM results have shown a few ciliated bipolar cells in mouse retinas. However, probably owing to microscope limitations, we failed to visualize cilia from bipolar and horizontal cells in mouse retina by immunostaining. It is possible, because of the features of cilia, that they are tiny and constantly disassemble and reassemble along the cell cycle. Hence, we cannot conclude that bipolar and horizontal cells are not ciliated.

In the inner retina, more than 45 different amacrine cell classes influence excitatory connections and postsynaptic inhibition.[35] We compared cilia profiles in different subtypes of amacrine cells in mice. The highest ciliation of amacrine cell subtypes is present in Prox1-positive amacrine cells, which is a marker for AII amacrine cells. AII amacrine cells transfer visual information from rod

to ganglion cells.[61] Interestingly, different subtypes show different ciliation. We expected it might be based on the different functions of subtypes. Because ciliary proteins and related signaling pathways are required for embryonic patterning in mouse brain,[8,9] we hypothesize that cilia in the INL may also play a role in retinal patterning during development, especially for amacrine cells. However, retinal structure analysis by OCT in Vift88 mice showed normal retinal structure and normal vision, tested by ERG. There may be several explanations as to why we did not observe any defect, the most obvious being the limitation of populations of vGluT3-expressing amacrine cells in mice. The total number of vGluT3-expressing amacrine cells varies across the mouse strains, from a low of approximately 10,400 cells per retina to a high of approximately 14,900 cells, as previously reported.[62] In rat retina, vGluT3-expressing amacrine cells are account for around 1% of the total amacrine cells.[63] We hypnotized that may be due to the small population of vGluT3-expressing amacrine cells, so that the phenotypes were not obvious in Vift88 mice. Removing cilia from more types of amacrine cells, such as AII amacrine cells may have more of an impact, because their populations were five to eight times more than the vGluT3-expressing amacrine cells population.[62] In addition, the unique function of VG3-amacrine cells is object motion detection, which may indicate that cilia have participated in part of the process. The further experiments related to direction and neuron processing are necessary to solve the puzzle.

A surprising finding here is that the ciliation profile of Müller glial cells varied significantly during different stages of development in the mouse eye, suggesting that primary cilia regulate the terminal differentiation and proliferation of this cell type. Müller glial cells are a unique retinal cell type because they are the only retinal cell known to have stem cell–like properties.[42] They may play a critical role in the regeneration of neuronal lineages, for example, after retinal injury. Thus, primary cilia, as known gatekeepers of the cell cycle, might contribute significantly to regulating these mechanisms.

Collectively, our study provides a comprehensive initial characterization of cilia distribution in the developing and mature mouse retina. Our findings highlight a possible role for the primary cilia of amacrine cells in regulating retinal development and maintenance. They may play a critical regulatory function in integrating visual signals, thus providing a platform for the development of potential future therapeutic approaches.

Disclosure: **K. Ning**, None; **B.E. Sendayen**, None; **T.J. Kowal**, None; **B. Wang**, None; **B.W. Jones**, None; **Y. Hu**, None; **Y, Sun**, None

References

1. Goetz SC, Anderson KV. The primary cilium: a signalling centre during vertebrate development. *Nat Rev Genet*. 2010;11:331–344.
2. Satir P, Christensen ST. Overview of structure and function of mammalian cilia. *Annu Rev Physiol*. 2007;69:377–400.
3. Patnaik SR, Kretschmer V, Brücker L, et al. Bardet-Biedl syndrome proteins regulate cilia disassembly during tissue maturation. *Cell Mol Life Sci*. 2019;76:757–775.
4. Singla V, Reiter JF. The primary cilium as the cell's antenna: signaling at a sensory organelle. *Science*. 2006;313:629–633.
5. Veland IR, Awan A, Pedersen LB, Yoder BK, Christensen ST. Primary cilia and signaling pathways in mammalian development, health and disease. *Nephron Physiol*. 2009;111:39–53.
6. Ning K, Song E, Sendayen BE, et al. Defective INPP5E distribution in NPHP1-related Senior-Loken syndrome. *Mol Genet Genomic Med*. 2020;9:e1566.
7. Green JA, Mykytyn K. Neuronal primary cilia: an underappreciated signaling and sensory organelle in the brain. *Neuropsychopharmacology*. 2014;39:244–245.
8. Guemez-Gamboa A, Coufal NG, Gleeson JG. Primary cilia in the developing and mature brain. *Neuron*. 2014;82:511–521.
9. Youn YH, Han YG. Primary cilia in brain development and diseases. *Am J Pathol*. 2018;188:11–22.
10. Alvarado JA, Dhande OS, Prosseda PP, et al. Developmental distribution of primary cilia in the retinofugal visual pathway. *J Comp Neurol*. 2020;529:1442–1455.
11. Hildebrandt F, Benzing T, Katsanis NC. Ciliopathies. *N Engl J Med*. 2011;364:1533–1543.
12. Wang SF, Kowal TJ, Ning K, et al. Review of ocular manifestations of Joubert syndrome. *Genes (Basel)*. 2018;9:605.
13. Waters AM, Beales PL. Ciliopathies: an expanding disease spectrum. *Pediatr Nephrol*. 2011;26, 1039–1056.
14. Ma X, Ning K, Jabbehdari S, et al. Oculocerebrorenal syndrome of Lowe: Survey of ophthalmic presentations and management. *Eur J Ophthalmol*. 2020;30:966–973.
15. Prosseda PP, Luo N, Wang B, et al. Loss of OCRL increases ciliary PI(4,5)P2 in Lowe oculocerebrorenal syndrome. *J Cell Sci*. 2017;130:3447–3454.
16. Burnett JB, Lupu FI, Eggenschwiler JT. Proper ciliary assembly is critical for restricting Hedgehog signaling during early eye development in mice. *Dev Biol*. 2017;430:32–40.
17. Lepanto P, Davison C, Casanova G, Badano JL, Zolessi FR. Characterization of primary cilia during the differentiation of retinal ganglion cells in the zebrafish. *Neural Dev*. 2016;11:10.
18. Braun DA, Hildebrandt FC. Ciliopathies. *Cold Spring Harb Perspect Biol*. 2017;9:a028191.
19. Hartill V, Szymanska K, Sharif SM, Wheway G, Johnson CA. Meckel-Gruber syndrome: an update on diagnosis, clinical management, and research advances. *Front Pediatr*. 2017;5:244.
20. Lee JE, Gleeson JG. A systems-biology approach to understanding the ciliopathy disorders. *Genome Med*. 2011;3:59.
21. Dyson JM, Conduit SE, Feeney SJ, et al. INPP5E regulates phosphoinositide-dependent cilia transition zone function. *J Cell Biol*. 2017;216:247–263.
22. May-Simera H, Nagel-Wolfrum K, Wolfrum U. Cilia – the sensory antennae in the eye. *Prog Retin Eye Res*. 2017;60:144–180.

23. Rachel RA, Li T, Swaroop A. Photoreceptor sensory cilia and ciliopathies: focus on CEP290, RPGR and their interacting proteins. *Cilia*. 2012;1:22.

24. Bujakowska KM, Liu Q, Pierce EA. Photoreceptor cilia and retinal ciliopathies. *Cold Spring Harb Perspect Biol*. 2017;9:a028274.

25. Chen HY, Welby E, Li T, Swaroop A. Retinal disease in ciliopathies: recent advances with a focus on stem cell-based therapies. *Transl Sci Rare Dis*. 2019;4:97–115.

26. Wheway G, Parry DA, Johnson CA. The role of primary cilia in the development and disease of the retina. *Organogenesis*. 2014;10:69–85.

27. Zhang Y, Williams PR, Jacobi A, et al. Elevating growth factor responsiveness and axon regeneration by modulating presynaptic inputs. *Neuron*. 2019;103:39–51.e35.

28. Allen RA. Isolated cilia in inner retinal neurons and in retinal pigment epithelium. *J Ultrastruct Res*. 1965;12:730–747.

29. Boycott BB, Hopkins JM. A neurofibrillar method stains solitary (primary) cilia in the mammalian retina: their distribution and age-related changes. *J Cell Sci*. 1984;66:95–118.

30. Kim YK, Kim JH, Yu YS, Ko HW, Kim JH. Localization of primary cilia in mouse retina. *Acta Histochem*. 2013;115:789–794.

31. O'Connor AK, Malarkey EB, Berbari NF, et al. An inducible CiliaGFP mouse model for in vivo visualization and analysis of cilia in live tissue. *Cilia*. 2013;2:8.

32. Euler T, Haverkamp S, Schubert T, Baden T. Retinal bipolar cells: elementary building blocks of vision. *Nat Rev Neurosci*. 2014;15:507–519.

33. Wan QF, Heidelberger R. Synaptic release at mammalian bipolar cell terminals. *Vis Neurosci*. 2011;28:109–119.

34. Balasubramanian R, Gan L. Development of retinal amacrine cells and their dendritic stratification. *Curr Ophthalmol Rep*. 2014;2:100–106.

35. Masland RH. The tasks of amacrine cells. *Vis Neurosci*. 2012;29:3–9.

36. Kim T, Soto F, Kerschensteiner D. An excitatory amacrine cell detects object motion and provides feature-selective input to ganglion cells in the mouse retina. *Elife*. 2015;4:e08025.

37. Lagnado L. Retinal processing: amacrine cells keep it short and sweet. *Curr Biol*. 1998;8:R598–R600.

38. Kunzevitzky NJ, Willeford KT, Feuer WJ, Almeida MV, Goldberg JL. Amacrine cell subtypes differ in their intrinsic neurite growth capacity. *Invest Ophthalmol Vis Sci*. 2013;54:7603–7613.

39. Yan W, Laboulaye MA, Tran NM, et al. Mouse retinal cell atlas: molecular identification of over sixty amacrine cell types. *J Neurosci*. 2020;40:5177–5195.

40. Chen M, Lee S, Zhou ZJ. Local synaptic integration enables ON-OFF asymmetric and layer-specific visual information processing in vGluT3 amacrine cell dendrites. *Proc Natl Acad Sci USA*. 2017;114:11518–11523.

41. Hsiang JC, Johnson KP, Madisen L, Zeng H, Kerschensteiner D. Local processing in neurites of VGluT3-expressing amacrine cells differentially organizes visual information. *Elife*. 2017;6:e31307.

42. Goldman D. Muller glial cell reprogramming and retina regeneration. *Nat Rev Neurosci*. 2014;15, 431–442.

43. Newman E, Reichenbach A. The Muller cell: a functional element of the retina. *Trends Neurosci*. 1996;19:307–312.

44. Ferraro S, Gomez-Montalvo AI, Olmos R, Ramirez M, Lamas M. Primary cilia in rat mature Muller glia: downregulation of IFT20 expression reduces sonic hedgehog-mediated proliferation and dedifferentiation potential of Muller glia primary cultures. *Cell Mol Neurobiol*. 2015;35:533–542.

45. Bangs FK, Schrode N, Hadjantonakis AK, Anderson KV. Lineage specificity of primary cilia in the mouse embryo. *Nat Cell Biol*. 2015;17:113–122.

46. Dhande OS, Stafford BK, Franke K, et al. Molecular fingerprinting of on-off direction-selective retinal ganglion cells across species and relevance to primate visual circuits. *J Neurosci*. 2019;39:78–95.

47. Anderson JR, Jones BW, Watt CB, et al. Exploring the retinal connectome. *Mol Vis*. 2011;17:355–379.

48. Anderson JR, Mohammed S, Grimm B, et al. The Viking viewer for connectomics: scalable multi-user annotation and summarization of large volume data sets. *J Microsc*. 2011;241:13–28.

49. Zhang J, Li L, Huang H, et al. Silicone oil-induced ocular hypertension and glaucomatous neurodegeneration in mouse. *Elife*. 2019;8:e45881.

50. Chou TH, Bohorquez J, Toft-Nielsen J, Ozdamar O, Porciatti V. Robust mouse pattern electroretinograms derived simultaneously from each eye using a common snout electrode. *Invest Ophthalmol Vis Sci*. 2014;55:2469–2475.

51. Manuel MN, Mi D, Mason JO, Price DJ. Regulation of cerebral cortical neurogenesis by the Pax6 transcription factor. *Front Cell Neurosci*. 2015;9:70.

52. Shaham O, Menuchin Y, Farhy C, Ashery-Padan R. Pax6: a multi-level regulator of ocular development. *Prog Retin Eye Res*. 2012;31:351–376.

53. Philips GT, Stair CN, Young Lee H, et al. Precocious retinal neurons: Pax6 controls timing of differentiation and determination of cell type. *Dev Biol*. 2005;279:308–321.

54. Ennis S, Kunz YW. Differentiated retinal Muller glia are ciliated–ultrastructural evidence in the teleost Poecilia reticulata P. *Cell Biol Int Rep*. 1986;10:611–622.

55. Nelson BR, Ueki Y, Reardon S, et al. Genome-wide analysis of Muller glial differentiation reveals a requirement for Notch signaling in postmitotic cells to maintain the glial fate. *PLoS One*. 2011;6:e22817.

56. Pellissier LP, Hoek RM, Vos RM, et al. Specific tools for targeting and expression in Muller glial cells. *Mol Ther Methods Clin Dev*. 2014;1:14009.

57. Poche RA, Furuta Y, Chaboissier MC, Schedl A, Behringer RR. Sox9 is expressed in mouse multipotent retinal progenitor cells and functions in Muller glial cell development. *J Comp Neurol*. 2008;510:237–250.

58. Sun W, Cornwell A, Li J, et al. SOX9 is an astrocyte-specific nuclear marker in the adult brain outside the neurogenic regions. *J Neurosci*. 2017;37:4493–4507.

59. Cherry TJ, Trimarchi JM, Stadler MB, Cepko CL. Development and diversification of retinal amacrine interneurons at single cell resolution. *Proc Natl Acad Sci USA*. 2009;106:9495–9500.

60. Kim DS, Ross SE, Trimarchi JM, et al. Identification of molecular markers of bipolar cells in the murine retina. *J Comp Neurol*. 2008;507:1795–1810.

61. Marc RE, Anderson JR, Jones BW, Sigulinsky CL, Lauritzen JS. The AII amacrine cell connectome: a dense network hub. *Front Neural Circuits*. 2014;8:104.

62. Keeley PW, Whitney IE, Madsen NR, et al. Independent genomic control of neuronal number across retinal cell types. *Dev Cell*. 2014;30:103–109.

63. Haverkamp S, Wassle H. Characterization of an amacrine cell type of the mammalian retina immunoreactive for vesicular glutamate transporter 3. *J Comp Neurol*. 2004;468:251–263.